Vascular Endothelial Growth Factor Mediates Corneal Nerve Repair

Charles Q. Yu,[1,2,3] *Min Zhang,*[1,2] *Krisztina I. Matis,*[1] *Charles Kim,*[1,3] *and Mark I. Rosenblatt*[1,3,4]

Purpose. To examine the expression of vascular endothelial growth factor (VEGF) and its receptors in the cornea and the trigeminal ganglion and to characterize the role of VEGF in mediating corneal nerve repair.

Methods. Regeneration of the corneal subbasal nerve plexus after epithelial debridement was measured. The expression of VEGF and its receptors was examined in the trigeminal ganglia and in the cornea by RT-PCR, immunohistochemistry, and Western blotting. VEGF-mediated nerve growth was measured in a trigeminal ganglia explant assay. Anti–VEGF neutralizing antibody was used to examine the VEGF-dependent growth of neurons in vitro and regeneration of the corneal nerves in vivo.

Results. After two distinct patterns of nerve regeneration, the subbasal nerves recovered to 65% of the preinjury density after 28 days. RT-PCR demonstrated gene expression of VEGF and VEGF receptors in the trigeminal ganglia. Immunohistochemistry showed staining for VEGF and its receptors in the trigeminal ganglia and for VEGFR1, VEGFR2, and neuropilin (NRP)-1 in the cornea. Western blot confirmed these results. In vitro, VEGF promoted the growth of explanted trigeminal ganglia by 91%. Blockage of VEGF signaling with anti–VEGF antibody reduced the growth of cultured neurons by 17% and the regeneration of subbasal neurons by 23%.

Conclusions. In addition to providing new information on the regeneration of murine corneal nerves, this study presents evidence that VEGF signaling influences the repair of corneal nerves by demonstrating that VEGF and VEGF receptors are present in the trigeminal ganglia and that abrogation of VEGF signaling reduces nerve growth in vitro and in vivo. (*Invest Ophthalmol Vis Sci.* 2008;49:3870–3878) DOI:10.1167/iovs.07-1418

From the [1]Department of Ophthalmology and Vision Science, University of California Davis School of Medicine, Sacramento, California; and [3]The Margaret M. Dyson Vision Research Institute and the [4]Department of Ophthalmology, Weill Cornell Medical College, New York, New York.

[2]Contributed equally to the work and therefore should be considered equivalent authors.

Supported by National Institutes of Health Grants K08EY015829 (MIR), R01DK069978, and R01DK052581 for gene expression core facilities; the Howard Hughes Medical Institute (CQY and CK are Medical Research Training Fellows); and an unrestricted grant from Research to Prevent Blindness.

Submitted for publication November 3, 2007; revised March 28, 2008; accepted July 2, 2008.

Disclosure: **C.Q. Yu**, None; **M. Zhang**, None; **K.I. Matis**, None; **C. Kim**, None; **M.I. Rosenblatt**, None

The publication costs of this article were defrayed in part by page charge payment. This article must therefore be marked "*advertisement*" in accordance with 18 U.S.C. §1734 solely to indicate this fact.

Corresponding author: Mark I. Rosenblatt, Margaret M. Dyson Vision Research Institute, Department of Ophthalmology, Weill Cornell Medical College, 1300 York Avenue, LC-305, New York, NY 10065; mar2058@med.cornell.edu.

The cornea, with primarily sensory and some autonomic innervation, is among the most densely innervated tissue of the human body.[1] In humans, most corneal nerves originate from the ophthalmic branch of the trigeminal nerve and form a subbasal plexus under the corneal epithelium. This plexus extends thin nerve leashes that contain nociceptors at the surface of the cornea.[2] Corneal nerves are of great importance because of their role in protecting the cornea from irritants and their trophic properties, which are necessary to maintain a healthy ocular surface.[3] Disruption of the corneal nerves has been shown to impair corneal healing significantly.[4]

Vascular endothelial growth factor (VEGF) has long been known as a potent growth factor that stimulates the proliferation of blood vessels. Specifically, it is an endothelial cell mitogen and angiogenic factor and a potent mediator of vascular permeability.[5] Signaling is mediated by the flt-1 (VEGFR1), flk-1 (VEGFR2), neuropilin (NRP)-1, and NRP2 receptors.[6] VEGF is essential for blood vessel development and has been strongly implicated in the pathogenesis of diabetic retinopathy, retinopathy of prematurity, age-related macular degeneration, and corneal neovascularization.[7–12] The healthy cornea has minimal free VEGF.[13] However, in injured states, VEGF expression has been shown to be upregulated and can contribute to corneal neovascularization.[14] Anti–VEGF therapies have become important tools in slowing the growth of some cancerous tumors and have been used to treat ocular diseases such as macular degeneration. Recently, investigators have shown that the anti–VEGF neutralizing antibody bevacizumab can bind murine $VEGF_{164}$ and human $VEGF_{165}$ and that topical or systemic application of bevacizumab inhibits inflammation-induced angiogenesis and lymphangiogenesis in the cornea.[15]

VEGF has also been implicated as an important player in nerve growth. In vitro experiments have shown that VEGF and its receptor are expressed by neurons and stimulate neurogenic, neuroprotective, and neurotrophic activities.[16–18] These activities include proliferation of cortical neurons, protection of central and peripheral neurons from hypoxia-induced death, and promotion of axonal outgrowth in peripheral neurons.[19] VEGF has also been shown to have an important role in neurodegenerative diseases such as amyotrophic lateral sclerosis.[20–22] Studies have indicated that systemic inhibition of VEGF with bevacizumab may cause apoptosis in retinal neurons.[23] However, implications for anti–VEGF therapy on corneal innervation or nerve repair have not been explored.

Here we used a transgenic mouse displaying corneal neurofluorescence[24] to characterize the pattern of nerve regeneration in the cornea after epithelial debridement. Then, with the use of RT-PCR, immunohistochemistry, and Western blot, we investigated the expression of VEGF ($VEGF_{164}$) and its receptors in the cornea and trigeminal ganglia. Last, we observed the effect of VEGF on trigeminal neuron outgrowth in vitro and the effects of anti–VEGF neutralizing antibodies on the axonal extension in vitro and on the regeneration of the subbasal nerve plexus after injury.

Investigative Ophthalmology & Visual Science, September 2008, Vol. 49, No. 9

Materials and Methods

Animal Model and Care

Neurofluorescent adult mice of the *thy1*-YFP line 16 were purchased from Jackson Laboratories (Bar Harbor, ME) and bred to homozygosity. For in vivo experiments, mice were anesthetized with intraperitoneal injections of a combination of ketamine (20 mg/kg; Phoenix Scientific, St. Joseph, MO) and xylazine (6 mg/kg; Phoenix Scientific). For terminal experiments, mice were killed with a lethal dose of intraperitoneal pentobarbital (100 mg/kg; Abbott Laboratories, North Chicago, IL). For immunostaining experiments, wild-type C57/BL6 mice were used to eliminate bleed-through from transgenic fluorescence. All animals were managed and experiments were conducted according to the ARVO Statement for the Use of Animal in Ophthalmic and Vision Research.

Fluorescence Imaging

Corneal whole mounts, trigeminal neuron cultures, and tissue slides were imaged with a fluorescence stereoscope (Stereolumar V.12; Carl Zeiss Meditec GmbH, Oberkochen, Germany) equipped with a digital camera (Axiocam MRm; Carl Zeiss Meditec GmbH) and a motorized fluorescence microscope (AxioVert 200M, with Axiovision 4.0; Carl Zeiss Meditec GmbH) equipped with a slider module (Axiocam MRm; Carl Zeiss Meditec GmbH) for optical sectioning controlled by the system software (Axiovision 4.0; Carl Zeiss Meditec GmbH).

Corneal Wounding and Regeneration

Mice were anesthetized, and a 2-mm circular corneal epithelial defect was made in each anesthetized mouse using a scalpel blade. At selected times after wounding, groups of mice were killed, and corneas were removed and fixed in 4% paraformaldehyde for 40 minutes. After four relaxing radial incisions were made, the corneas were coverslipped with mounting medium containing DAPI (4′, 6′-diamino-2-phenylindole; Vector Laboratories, Burlingame, CA) and were imaged. Samples were masked, and four photographs (390 μm $\times$ 220 μm), one at the center of each quadrant of the cornea in the area of the wound, were taken. Nerve fibers were traced, and the length was calculated with commercial software (Adobe Illustrator; Adobe Systems, San Jose, CA) with an object-length function.[24] The lengths of nerve processes found were totaled and converted to micrometers of nerves per square millimeter. The density of the nerves at each time point was then charted as a percentage of control.

Trigeminal Neuronal and Cornea Epithelial Cell Cultures

Trigeminal ganglia were removed from mice and cultured, as has been previously described.[24] Cultures were maintained in 96-well plates coated with 20 μg/mL laminin (Sigma, St. Louis, MO) and supported with media (Neurobasal; Invitrogen, Carlsbad, CA) supplemented with 2% fetal bovine serum (FBS) and 1% antibiotic/antimycotic (ABAM; Gibco, Grand Island, NY).

Mouse corneal epithelial sheets were isolated using dispase treatment, as described by Kawakita et al.[25] Epithelial sheets were rendered into single cells by 0.25% trypsin-EDTA (Gibco). Single cells were seeded in six-well plates with corneal epithelium growth medium (Epilife; Cascade Biologics, Portland OR) with 20 μM calcium, 1% human corneal growth supplement (Cascade Biologics), 0.01 μg/mL mouse epidermal growth factor (Sigma), 10^{-7} mM cholera toxin A subunit from *Vibrio cholerae* (Sigma), and 1% ABAM (Gibco) until they were 90% confluent.

Immunohistochemistry of VEGF and Receptors in Trigeminal Cultures and Whole Tissue

Trigeminal neuron cultures were collected from nonfluorescent C57/BL6 mice to avoid fluorescence bleed-through during imaging.[6] Neuronal cells were fixed in 2% paraformaldehyde for 20 minutes, followed by phosphate-buffered saline (PBS) washing. The cells were then permeablized and blocked with 1% bovine serum albumin and 0.1% Triton-X in PBS for 30 minutes After blocking, the following primary antibodies were applied to individual wells: rabbit anti-$VEGF_{164}$ (1:200); goat anti-VEGFR1 (1:200); goat anti-VEGFR2 (1:200); rabbit anti-NRP1 (1:200); and rabbit anti-NRP2 (1:200; Santa Cruz Biotechnology, Santa Cruz, CA). Cells were washed with PBS before the application of the secondary antibody (45 minutes), donkey anti-rabbit and donkey anti-goat (1:300; Jackson ImmunoResearch, West Grove, PA). Finally, neuronal cultures were rinsed with PBS, mounted in media containing DAPI, and coverslipped for imaging.

Whole trigeminal ganglia and corneas were collected from C57/BL6 mice, fixed in 4% paraformaldehyde for 45 minutes, embedded in optimal cutting temperature (OCT; Tissue-Tek, Torrance, CA) media, and frozen on dry ice. Cross cryosections 8-μm thick were cut and mounted on glass slides (R7200; Mercedes Medical, Sarasota, FL). Sections were blocked and permeabilized with 1-hour incubation in 1% bovine serum albumin (Sigma) in PBS with 0.1% Triton X-100. Sections were incubated overnight with the following antibodies: rabbit anti-$VEGF_{164}$ (1:200); goat anti-VEGFR1 (1:200); goat anti-VEGFR2 (1:200); rabbit anti-NRP1 (1:200); and rabbit anti-NRP2 (1:200) (all from Santa Cruz Biotechnology). Slides were washed with PBS and incubated in donkey anti–rabbit and donkey anti–goat (both 1:500) secondary antibody (Jackson ImmunoResearch) for 6 hours. Slides were then washed and mounted in media and coverslipped for imaging.

RT-PCR of Corneal Epithelial and Trigeminal Whole Tissue and Cultures

Total RNA was isolated (RNeasy Mini Kit and RNeasy Micro Kit; Qiagen, Germantown, MD) from five sources—mouse cultured corneal epithelial cells (passage 0), cultured trigeminal neurons (passage 0), cornea epithelial tissue, cornea stroma tissue, and trigeminal ganglion tissue—according to the manufacturer's protocol. Mouse embryos (embryonic day [E] 11.5) were used as a positive control. RNase-free DNaseI was used to remove DNA. RNA was stored at −70°C in the presence of RNase inhibitor (Invitrogen, Carlsbad, CA), and RNA concentration and quality were assessed (2100 Bioanalyzer; Agilent, Santa Clara, CA).

cDNA was generated (Superscript III First-Strand Synthesis System; Invitrogen) according to the manufacturer's protocols. Total RNA (500–1000 ng) was reverse transcribed (Oligo(dT)20; Invitrogen). Of the resultant cDNA, 50 ng was used for each PCR amplification, in accordance with the manufacturer's protocol (MasterTaq Kit; Eppendorf, Hamburg, Germany). Specific primers were designed [26,27] as follows: $VEGF_{164}$ forward (5′-CAGGCTGCTGTA ACGATGAA-3′) and reverse (5′-CACCGCCTTGGCTTGTCACA-3′), VEGFR1 forward (5′-GAGAGCATCTATAAGGCAGCGGATT-3′) and reverse (5-CACGTT-TACAAT GAGAGTGGCAGTG-3′), VEGFR2 forward (5′-TACACAAT-TCAGAGCGATGTGTGGT-3′) and reverse (5′-CTGGTTCCTCCAATGG-GATATCTTC-3′), NRP1 forward (5′-GAAGGCAACAACAACTA TGA-3′) and reverse (5′-ATGCTCCCAGTG GCAGAATG-3′), NRP2 forward (5′-AAGTGGG GGAAGGAGACTGT-3′) and reverse (5′-GTC CACCTC-CCATCAGAGAA-3′), and GAPDH control forward (5′-ACCACAGTC CATGCC ATCAC-3′) and reverse (5′-TCCACCACCCTGT TGCTGTA-3′). Amplifications were performed using the following cycling parameters: 94°C for 3 minutes, followed by 30 cycles of 94°C for 45 seconds, annealing temperature ($VEGF_{164}$, VEGFR1, VEGFR2, 53.4°C; NRP1, 55.7°C; NRP2, 61°C; GAPDH, 60°C) for 30 seconds and 72°C for 45 seconds, and a final extension cycle of 72°C for 5 minutes.[26] Glutaraldehyde phosphate dehydrogenase was the loading control. A negative control without cDNA was also performed (data not shown). PCR products were resolved in 1.5% agarose gels.

Western Blot Analysis

Whole trigeminal ganglia and corneas from C57/BL6 mice were frozen in liquid nitrogen and homogenized using RIPA buffer (10 mM Tris-HCl, 150 mM NaCl, 1% deoxycholic acid, 1% Triton X-100, 0.1% SDS,

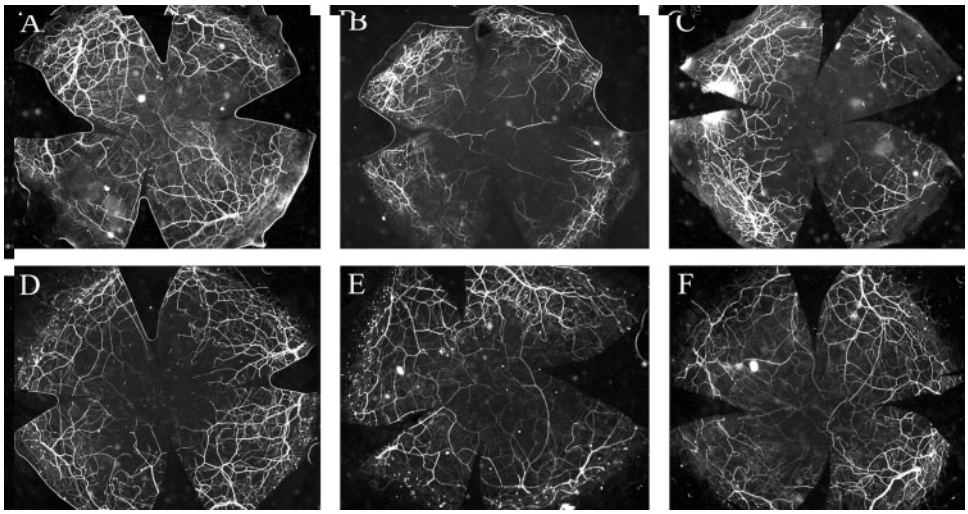

FIGURE 1. Regeneration of mouse corneal subbasal nerve plexus density after wounding. Mice were separated into six groups ($n = 3$). Five groups underwent 2-mm–diameter circular superficial keratectomy. A control group received no injury. Mice were killed, and corneas were excised and imaged for neurofluorescence before injury (**A**), immediately after injury (**B**), and at 3 days (**C**), 7 days (**D**), 14 days (**E**), and 28 days (**F**) after initial wounding. The superficial wound removed all fibers of the subbasal plexus. Subsequently, a time-dependent increase in neuron density in the area of the wound could be observed. (For high-magnification images of corneas, see Figure 2.)

and 1 mM EDTA) containing 1 mM phenylmethylsulfonyl fluoride. After homogenization, the mixture was centrifuged and lysates were collected. Proteins were separated on 4% to 20% SDS-PAGE gel (Lonza, Visp, Switzerland). Proteins were transferred by electrophoresis onto polyvinylidene difluoride membranes and blocked in 3% BSA in PBS with 0.05% Tween 20. After blocking, the following concentration of antibodies was diluted in blocking solution and applied to each membrane for 90 minutes: rat anti-$VEGF_{164}$ (1:1000; R&D Systems, Minneapolis, MN); rabbit anti-VEGFR1 (1:2500, ab32152; Abcam, Cambridge, MA); rabbit anti-VEGFR2 (1:500, ab42230; Abcam); and rabbit anti-NRP1 (1:200) and rabbit anti-NRP2 (1:200) (H-286 and H-300; Santa Cruz Biotechnology). After washing in PBS with 0.15% Tween 20, blots were incubated with infrared-tagged anti–rat or anti–rabbit donkey secondary antibodies (1:1000; Rockland, Gilbertsville, PA) in blocking solution for 1 hour. Blots were analyzed with an imaging system (Odyssey Infrared; Li-Cor, Lincoln, NE). Negative controls omitted primary antibody.

Trigeminal Ganglion Explant Assay

Whole trigeminal ganglia were harvested from mice. Each ganglion was mounted in 7 μL basement membrane preparation (Matri-Gel; BD Biosciences, Franklin Lakes, NJ) to a well of a 48-well culture plate.[16] Ganglia were then incubated in 1 mL media (Neurobasal; Invitrogen) with 1% B27 supplement. For each pair, one ganglion served as control and the contralateral ganglion was treated with media containing 50 ng/mL VEGF. Media were changed every 3 days. After 6 days' growth at 37° and 5% CO_2, media were removed from wells, ganglia were fixed with 4% paraformaldehyde, and nerve outgrowths were visualized with anti-β III tubulin–specific antibody (Santa Cruz Biotechnology). Samples were masked, and three random fluorescence images (550 μm $\times$ 420 μm) of nerve outgrowth at the periphery of each ganglion were taken. Nerve densities for each set of ganglia were calculated and averaged.

Neuronal Growth Assay

Trigeminal ganglia were removed from mice, and neurons were dissociated and plated in 96-well glass culture plates as previously described. Cells were grown in media (Neurobasal; Invitrogen) with 2% FBS and 1% ABAM. Control samples were incubated in 250 ng/mL mouse IgG (Jackson ImmunoResearch), whereas experimental samples were exposed to 250 ng/mL bevacizumab (Genentech, South San Francisco, CA). After 48 hours of growth at 37°C and 5% CO_2, media were removed from the wells, and the cells were fixed in 2% paraformaldehyde for 20 minutes. The cells were then permeabilized with PBS containing 0.1% Triton X-100 and blocked with 1% BSA in PBS. Cells were incubated with anti-β III tubulin primary antibody at 1:2000 for 1 hour at room temperature, followed by detection using secondary antibody conjugated with Texas Red at 1:300 for an additional hour at room temperature. Samples were masked, and a fluorescence image (280 μm $\times$ 220 μm) was taken at the center of each quadrant of each well. Neuron axon lengths in each photograph were calculated.

Intrastromal Application of Anti–VEGF Blocking Antibody

Thy1-YFP mice were anesthetized, and a stromal micropocket extending from the limbus to the central cornea was created with a beveled needle (Microliter 701; Hamilton, Reno, NV). A syringe with a blunt 26-gauge needle was then used to inject 5 μL of 25 mg/mL bevacizumab or 5 μL of 25 mg/mL nonspecific mouse IgG in balanced salt solution into this pocket, which resulted in central hydration of the cornea. Twenty-four hours after intrastromal injection, the previously injected corneas were wounded, as described. Mice were killed 3 days after wounding, and the degree of nerve regeneration was quantified as in previous wounding experiments.

Statistical Analysis

Student's *t*-test was used, with statistical significance defined as $P < 0.05$.

RESULTS

Cornea Wounding and Regeneration of Nerves

Epithelial debridement with a scalpel blade was used to injure the corneas of *thy1*-YFP mice and resulted in the removal not only of the corneal epithelium but also of corneal nerves from the surface, including intraepithelial and subbasal plexus neurons. We have previously developed methods to quantify the density of the subbasal nerve plexus in these mice using endogenous neurofluorescence.[24] Corneal nerve regeneration after injury was monitored over time ($n = 3$ per time point). Starting from a control fluorescent nerve density of 53,173 $\pm$ 5408 (SEM) μm/mm^2, nerves recovered to densities of 31% (16,343 $\pm$ 742 μm/mm^2) at 3 days, 43% (23,114 $\pm$ 327 μm/mm^2) at 7 days, 57% (30,503 $\pm$ 2895 μm/mm^2) at 14 days, and 65% (34,476 $\pm$ 4648 μm/mm^2) at 28 days after injury (Figs. 1, 2).

Subbasal nerve regeneration took on two general forms. In some instances, the new nerves in the subbasal plexus emanated from fibers just outside the area of epithelial debridement (Fig. 3A). These appeared to represent extensions of already existing subbasal nerves. A second set of nerves regenerated as new

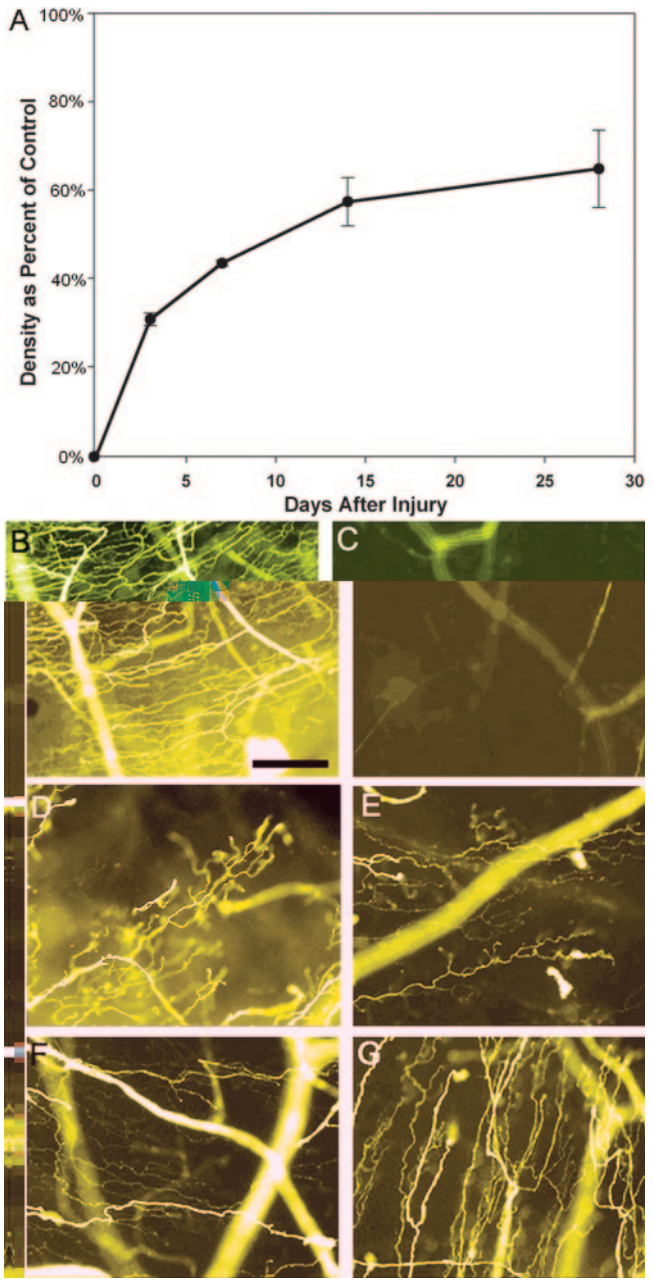

FIGURE 2. Quantification of the recovery of the subbasal nerve plexus after superficial injury using transgenic neurofluorescence. Photographs were taken in each of four quadrants of the corneas collected in the previous experiment (Fig. 1). The density of the subbasal nerve plexus was calculated and charted (mean ± SEM) as a percentage of control density (**A**). Representative fluorescence images from each time point are shown in (**B**) unwounded subbasal plexus, (**C**) plexus immediately after wounding, (**D**) plexus 3 days after wounding, (**E**) plexus 7 days after wounding, (**F**) plexus 14 days after wounding, and (**G**) plexus 28 days after wounding. The data show that at the area of de-epithelialization, nerve density recovers to approximately half the original density after 2 weeks and then plateaus to approximately 65% of prewounding levels. Scale bar, 100 μm.

"islands" of subbasal nerves that sprouted from deep stromal nerve bundles and had not been wounded (Fig. 3B).

Immunochemistry of VEGF and Receptors

To determine whether trigeminal neurons expressed the signaling components required for VEGF-dependent growth, we used immunostaining to examine the protein expression of VEGF and its receptors in cultured trigeminal neurons and in whole trigeminal tissue. In culture, processes and cell bodies of trigeminal nerves displayed strong staining for VEGF and NRP1 and moderately intense staining for VEGFR1 and VEGFR2. Minimal staining of NRP2 was found (Fig. 4).

In fixed trigeminal tissue sections, immunohistochemistry for $VEGF_{164}$ revealed a punctate pattern along with staining in processes and cell bodies. VEGFR1 staining was found in cell bodies, whereas VEGFR2 showed a striped pattern around cell bodies but little staining otherwise. Strong NRP1 staining was found in processes and cell bodies, but NRP2 showed only slight staining in cell bodies (Fig. 5).

In fixed corneal tissue, VEGFR1 and NRP1 showed strong staining in the epithelium. Notably, NRP1 had an intense perinuclear pattern of staining. VEGFR2 was weakly expressed in the epithelium, and VEGF and NRP2 displayed negligible staining (Fig. 6).

RT-PCR for VEGF and Its Receptors in Epithelium and Trigeminal Ganglia

To characterize the gene expression of VEGF ligands and receptors in the mouse cornea and trigeminal ganglion cells and tissues, semiquantitative RT-PCR techniques were used (Fig. 7). Intense bands corresponding to gene expression of VEGF, NRP1, NRP2, VEGFR1, and VEGFR2 were observed in cultured trigeminal neurons, whole trigeminal ganglia tissues, and corneal epithelial cells. In corneal epithelial tissue, less intense bands for VEGF and NRP1 were seen, whereas NRP2, VEGFR1, and VEGFR2 did not appear to be expressed at detectable levels. In the corneal stroma, only VEGF, VEGFR2, and NRP1 were detected as faint bands. NRP2 and VEGFR1 were not detected.

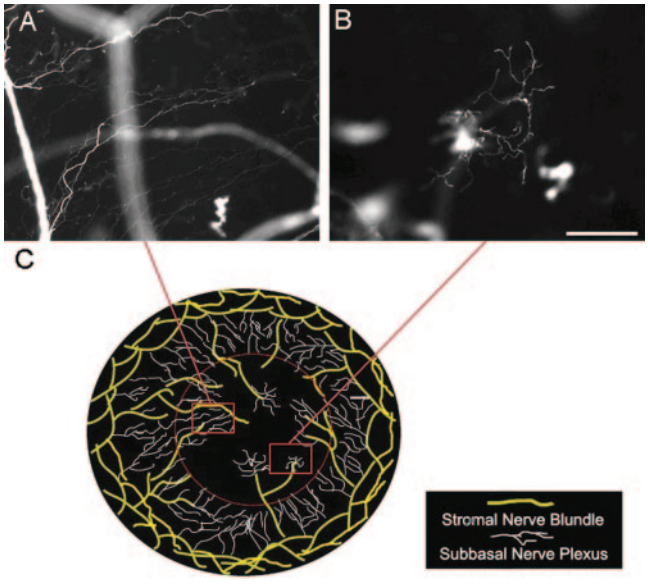

FIGURE 3. Two patterns of subbasal plexus nerve regeneration after injury. Detailed images (**A**, **B**) and a schematic drawing of wounded mouse cornea (**C**) depict two ways by which the mouse cornea regenerates its subbasal plexus after injury. *Red circle*: site of epithelial debridement and subbasal plexus destruction. Corneal stroma nerve bundles (*yellow*), which are deep in the cornea, are uninjured by epithelial debridement, whereas the thin subbasal plexus nerves (*white*) are removed by corneal abrasion and then subsequently heal. Some subbasal plexus nerves proximal to the area of abrasion grow back to reinnervate the cornea (**A**), whereas other "islands" of new subbasal plexus nerves grow from deep stroma nerves and then spread out (**B**). Scale bar, 100 μm.

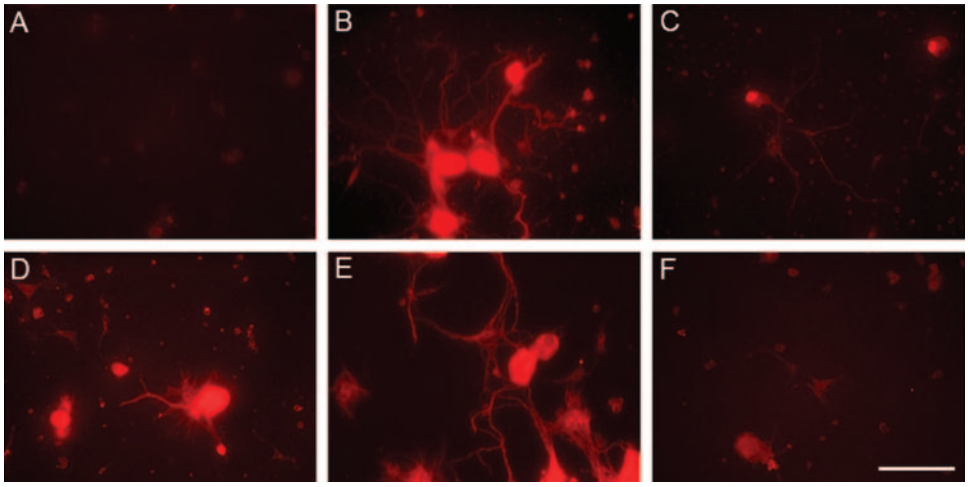

FIGURE 4. Immunocytochemistry for VEGF and VEGF receptors in trigeminal neurons. Primary cultures of trigeminal neurons were analyzed by immunocytochemistry for (**A**) negative control, (**B**) $VEGF_{164}$, (**C**) VEGFR1, (**D**) VEGFR2, (**E**) neuropilin-1, and (**F**) neuropilin-2. $VEGF_{164}$ and NRP1 were most highly expressed, followed by VEGFR2 and VEGFR1. NRP2 showed little expression. Scale bar, 100 μm.

Western Blot Analysis

To confirm the results of immunohistochemistry, Western blot analysis was conducted on whole trigeminal and corneal tissue. Immunoblotting of trigeminal tissue lysate showed positive reactivity for VEGF and its receptors. VEGF was present as band sizes of approximately 14 kDa, 18 kDa, and 23 kDa. VEGF receptors, including VEGFR1 (180-kDa band), VEGFR2 (220-kDa band), NRP1 (90-kDa band), and NRP2 (70-kDa band), were also expressed. Similarly, VEGFR2 and NRP1 were expressed in corneal tissue lysate. VEGFR1 was present as a 60-kDa band corresponding to soluble VEGFR1. However, corneal expression of VEGF and NRP2 proteins were not detected. These bands corresponded in size to previously published data on VEGF and its receptors and to data from the respective manufacturers (Fig. 8).[13,28,29]

In Vitro Effects of VEGF on Trigeminal Ganglia Explant Cultures

After 6 days' growth, extensive neurites had extended from the whole ganglia to the surrounding well. The density of these neuron outgrowths was photographed and quantified. In whole trigeminal explants mounted in basement membrane preparation (Matri-Gel; BD Biosciences), those treated with 50 ng/mL VEGF ($n = 5$) grew to a density of 71,060 ± 10,656 (SEM) μm/mm^2 after 6 days, and those without VEGF ($n = 5$) grew to a density of 37,268 ± 6943 μm/mm^2 ($P < 0.03$). This represented an increase of 90.6% over control (Fig. 9).

Effects of VEGF Inhibition on Corneal Nerves

After 48 hours of incubation with 2% serum, cultures of dissociated trigeminal neurons showed extensive axon outgrowth that extended over the surface of the well. The density of axons in wells with ($n = 4$) and without ($n = 4$) bevacizumab was quantified. Those treated with bevacizumab grew to a density of 63,862 ± 1409 (SEM) μm/mm^2, and those treated with IgG grew to a density of 76,837 ± 2574 μm/mm^2 ($P = 0.0045$). This represented a decrease of 16.9% compared with control (Fig. 10).

In living mice 3 days after epithelial debridement, those treated with bevacizumab ($n = 7$) recovered to a nerve density of 12,328 ± 845 μm/mm^2, and those treated with nonspecific mouse IgG ($n = 8$) recovered to a density of 15,939 ± 1141 μm/mm^2 (Fig. 11). This represented a significant decrease of 22.7% compared with control ($P < 0.03$).

DISCUSSION

Corneal nerve repair models after several types of injuries, including cryodamage, excimer laser ablation, and chemical injury, have been previously examined.[30–33] In our experiments, we charac-

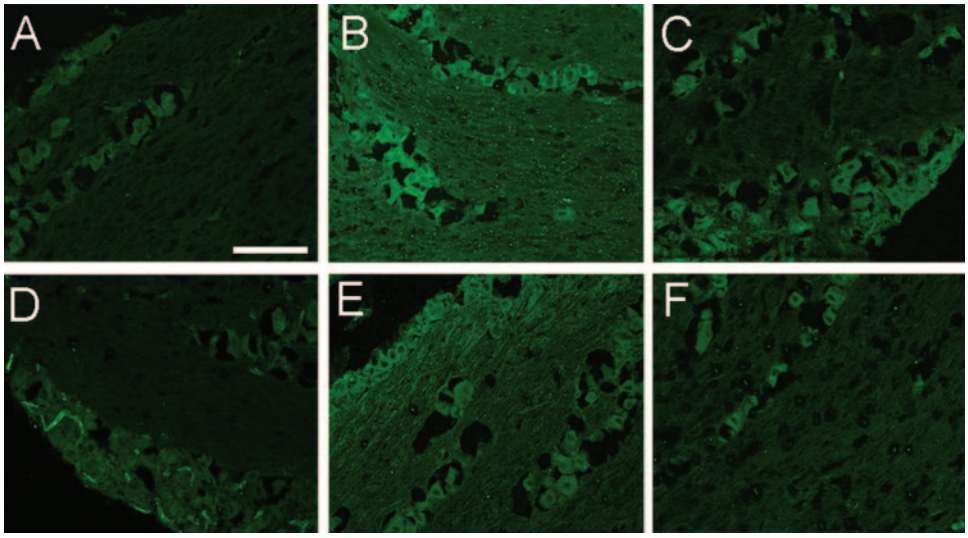

FIGURE 5. Immunohistochemistry for VEGF and its receptors in the trigeminal ganglion. Whole trigeminal neurons were analyzed by immunohistochemistry for (**A**) negative control, (**B**) $VEGF_{164}$, (**C**) VEGFR1, (**D**) VEGFR2, (**E**) neuropilin-1, and (**F**) neuropilin-2. Tissue cross-sections showed punctate pattern and staining in processes and cell bodies for VEGF. VEGFR1 staining was found in cell bodies. VEGFR2 showed a striped pattern around cell bodies but little staining otherwise. NRP1 staining was found in processes and cell bodies. NRP2 showed only minimal staining in cell bodies. Scale bar, 100 μm.

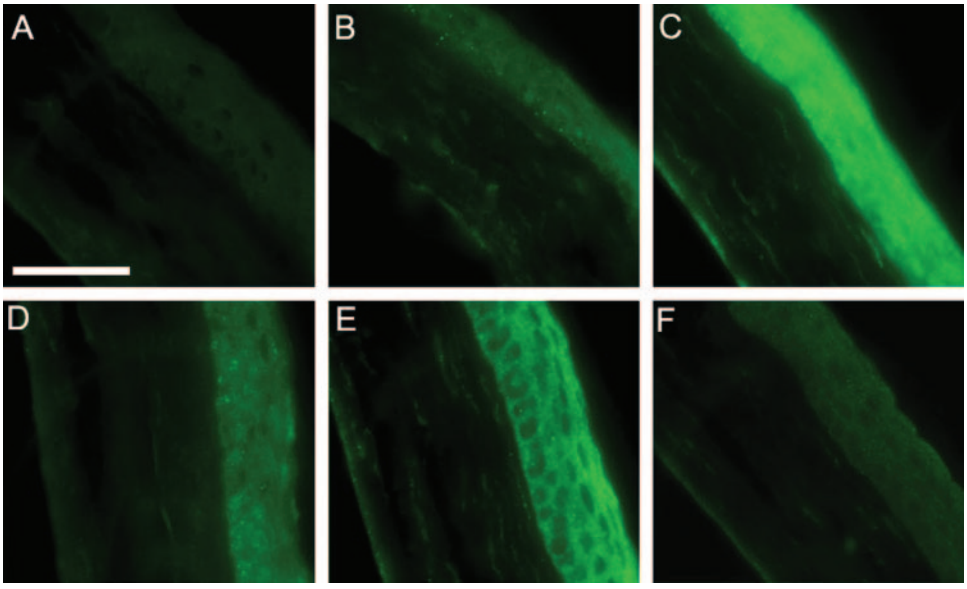

FIGURE 6. Immunohistochemistry for VEGF and its receptors in the cornea. Corneas were immunostained for (**A**) negative control, (**B**) $VEGF_{164}$, (**C**) VEGFR1, (**D**) VEGFR2, (**E**) neuropilin-1, and (**F**) neuropilin-2. VEGFR1 and NRP1 showed strong staining in the epithelium, and NRP1 also had a distinct perinuclear staining pattern. VEGFR2 showed some staining in the epithelium. $VEGF_{164}$ and NRP2 showed almost no staining. Scale bar, 50 μm.

terized manual debridement of the corneal epithelium as a nerve damage model. Although less invasive than some other models, we found that epithelial debridement also causes profound injury to nerves of the subbasal plexus. Importantly, the model recapitulates many of the nerve damage elements found clinically in common injuries such as corneal abrasions and loss of epithelium after surgical procedures (photorefractive and phototherapeutic keratectomy). Notably, a "gentler" disruption of the subbasal plexus avoids confounding variables such as the profound inflammation that occurs with cryodamage, the activation of stromal cells seen with photoablation, and the neovascularization seen in many other models.

We found that corneal subbasal nerve density regenerates quickly after wounding but plateaus after the first 2 weeks. The density did not return to prewounding levels even after 1 month. This rate of regeneration correlates well with previous studies that show approximately 60% of sensation restored in rabbits after 2 weeks.[34] It appears the density may level off at approximately 70% of the original. A 30% reduction in nerve density could result in loss of trophic influences and sensation that would hinder epithelialization and protection of the cornea. Whether this density eventually returns to prewounding levels and whether it is correlated with a loss of function has not been examined in our model, but results from previous studies in rabbits suggest that full function is not restored in the short term (10 weeks).[34]

Our results also showed two different sources of subbasal nerve plexus regeneration: from preexisting subbasal nerves and from islands originating from deeper bundles of nerves in the stroma. These two patterns of nerve regeneration were also seen in a rabbit model of corneal nerve cryoablation.[31] The contribution of these anterior stromal nerve fibers to the restoration of subbasal nerve density provides further evidence of the importance of these deeper nerves. Loss of the deeper nerves, which may serve as reservoirs for corneal surface nerve regeneration as occurs in ophthalmic procedures such as keratoplasty and LASIK, may therefore have significant implications for the restoration of subbasal nerve density and poten-

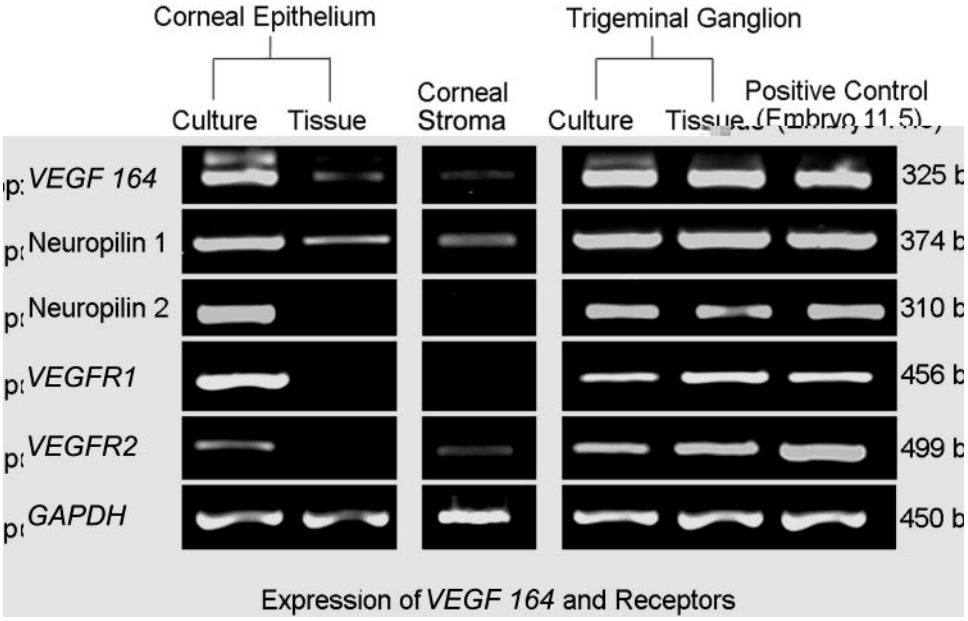

FIGURE 7. Semiquantitative RT- PCR of trigeminal ganglia and cornea for VEGF and VEGF receptors. Cultured trigeminal ganglia and corneal epithelial cells, cornea stroma tissue, and whole trigeminal ganglia tissue and corneal epithelial tissue were analyzed by RT-PCR for gene expression of *$VEGF_{164}$*, *NRP1*, *NRP2*, *VEGFR1*, and *VEGFR2*. Positive control was 11.5-day-old embryo. *$VEGF_{164}$* and *NRP1* genes appeared to be expressed in all sample tissues, though the bands were less bright in the corneal epithelial whole tissue and stroma. NRP2 and VEGFR1 were detected in all samples except corneal epithelial whole tissue and corneal stroma. VEGFR2 was detected in all samples except corneal epithelial whole tissue. GAPDH was used as a loading control.

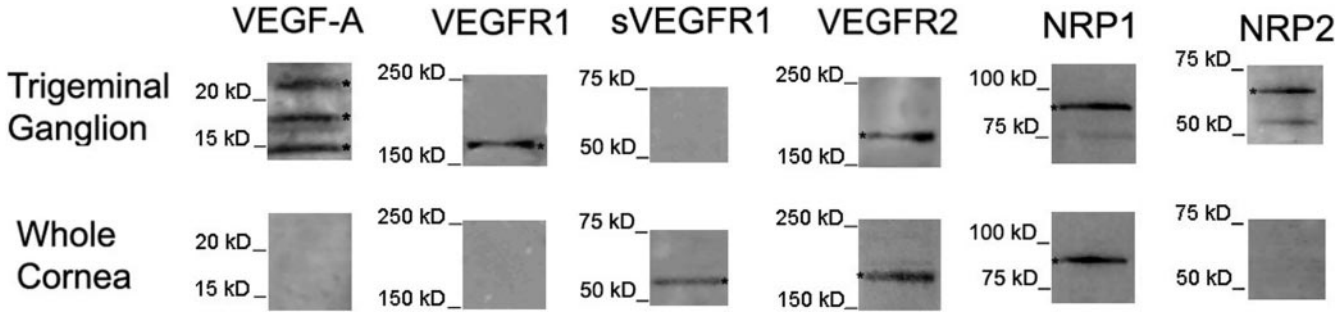

FIGURE 8. Analysis of VEGF and VEGF receptor protein expression by Western blot. Immunoblotting indicates protein expression of VEGF and its receptors in the trigeminal and of some VEGF receptors in the cornea. In the trigeminal ganglia, bands positive for VEGF were present at 14 kDa, 18 kDa, and 23 kDa. VEGFR1 was present at 180 kDa, VEGFR2 was present at 220 kDa, NRP1 was present at 90 kDa, and NRP2 was present at 70 kDa. Similar results were found in the cornea, but the VEGFR1-positive band corresponded in size (~60 kDa) to soluble VEGFR1. VEGF and NRP2 were not detected.

tially corneal sensation. We showed *thy1*-YFP neurofluorescent mice are an effective and expedient alternative to traditional techniques of corneal nerve visualization, such as gold chloride and specific antibody staining for nerve-specific ligands.[35]

We demonstrated by PCR that the trigeminal ganglion expresses some VEGF and VEGF receptor genes. Western blot analysis, in addition, confirmed immunochemistry findings of protein expression of VEGF and its four receptors in the trigeminal ganglion and of VEGFR1, VEGFR2, and NRP1 in the cornea. This shows that trigeminal neurons have the receptors able to detect and respond to VEGF in vivo. Although the neurons would in theory be the target of VEGF action, data indicate that they also secrete VEGF, demonstrating the potential action of VEGF in a paracrine or an autocrine fashion. Thus, VEGF may have an important role during the healing of the cornea, possibly promoting or guiding nerve growth.

We saw that giving 50 ng/mL VEGF, a concentration similar to what was used by other investigators[36,37] to induce angiogenesis, to trigeminal explants nearly doubled the nerve density of neuronal outgrowths after 6 days compared with control. Though neuron-promoting actions of VEGF have been shown in other nerves, such as those of the dorsal root ganglion, we are the first to find that such an effect occurs in trigeminal neurons. Additionally, such a profound increase in neuronal density suggests that VEGF may have an even more prominent role in nerve signaling and growth than previously thought.

To assess whether VEGF not only has the potential to stimulate trigeminal neurons but also plays a role in the growth and regeneration of neurons under physiological or pathophysiological conditions, we used bevacizumab to block its actions in vivo and in vitro. Inhibition of VEGF reduced the serum-dependent growth of cultured neurons by 17%. More important, adding anti–VEGF neutralizing antibodies to corneas undergoing subbasal nerve plexus regeneration inhibited the repair of these neurons by 23%. The role of VEGF signaling in corneal angiogenesis has been studied extensively, but these studies provide the first direct evidence that VEGF signaling also influences the repair of corneal nerves after injury. It should be noted that bevacizumab has a higher affinity for human VEGF than mouse VEGF; hence, these effects may be different and perhaps even greater in humans.[38]

Although we did not examine the corneal sensation of mice with and without treatment with bevacizumab after wounding, it can be expected that a lower nerve density would lead to at least some amount of impairment in function. Anti–VEGF neutralizing antibodies have been used extensively in the treatment of vitreoretinal diseases such as age-related macular de-

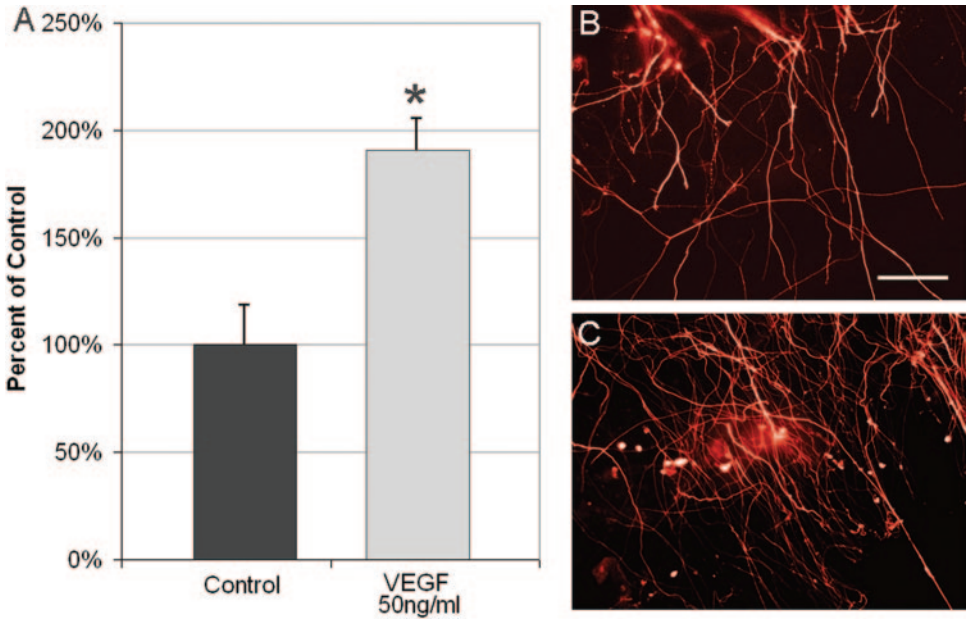

FIGURE 9. Effect of VEGF on outgrowth of explanted trigeminal ganglia. Whole trigeminal explants were collected from mice and mounted in basement membrane preparation (Matri-Gel; BD Biosciences). Half the samples ($n = 5$) were treated with 50 ng/mL VEGF (**C**), and the other half ($n = 5$) were given identical media that did not contain VEGF. After 6 days' growth, extensive neurites had extended from the whole ganglia to the surrounding plastic of the media well. These nerve outgrowths were photographed after nerve-specific immunostaining and were quantified. Those treated with VEGF (**C**) grew to a density of 71,060 ± 10,656 $\mu m/mm^2$ after 6 days, whereas those without VEGF (**B**) grew to a density of 37,268 ± 6943 $\mu m/mm^2$, representing an increase of 91% ($P < 0.03$). (**A**) Data are plotted as a percentage of control. *Asterisk*: statistical significance with $P < 0.05$. Scale bar, 100 μm.

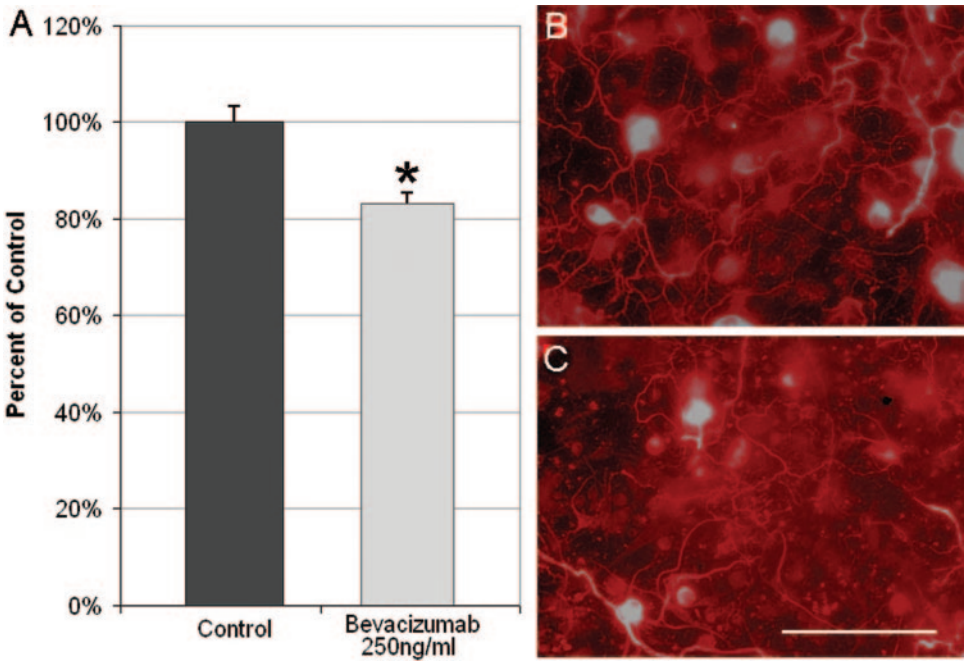

FIGURE 10. Effect of anti–VEGF antibody on axon outgrowth in dissociated trigeminal ganglia neurons. Cultures of dissociated neurons were grown with 2% serum and 250 ng/mL bevacizumab or 250 ng/mL mouse IgG for 48 hours. Cultures were then visualized with nerve-specific antibodies, and the density of nerve processes was quantified. Those with bevacizumab (**C**; $n = 4$) grew to a density of 63,862 ± 1409 $\mu m/mm^2$, whereas those treated with an equal amount of nonspecific IgG (**B**; $n = 4$) grew to a density of 76,837 ± 2574 $\mu m/mm^2$, representing a reduction in nerve density of 16% ($P < 0.005$). (**A**) Data are plotted as a percentage of control. *Asterisk*: statistical significance with $P < 0.05$. Scale bar, 100 μm Scale bar, 100 μm.

generation. However, preliminary investigations of bevacizumab as a treatment for corneal neovascularization are under way.[15] Given the finding that VEGF signaling modulated corneal nerve repair, further investigation of the antineuronal effects of antiangiogenesis treatment in the cornea is warranted. Indeed systemic administration of bevacizumab has been shown to cause a decrease in the numbers of retinal ganglion cells in vivo.[23]

The cornea is a unique tissue that is both highly innervated and avascular. The role of VEGF in corneal nerve maintenance has not been examined in the same way that quenching of VEGF signaling has been implicated for the maintenance of avascularity.[13,39] However, our data suggest that VEGF does play a role during the regeneration of corneal nerves, even in a model that does not generate neovascularization. It is possible the same decoy mechanisms, such as soluble VEGFR1 receptor, that affect angiogenesis help to regulate and modulate the effect of VEGF on corneal nerves. In the healthy cornea, these mechanisms may quench excessive nerve growth; however, in the injured cornea, downregulation of VEGF quenching is possible, thus promoting neurogenesis in the healing cornea. Additional studies will be required to ascertain how VEGF in the cornea can promote nerve growth while avoiding neovascularization. One possibility would be the existence of two different pathways for signaling by VEGF, one for vessel growth and permeability and another for mediating the neurotrophic effects. Other possibilities might include a differential VEGF dose dependence or different effective local concentrations of ligands and receptors between vascular and neuronal cell types.

Given our findings, we speculate that the VEGF affecting corneal nerves may be paracrine in nature. In addition, because

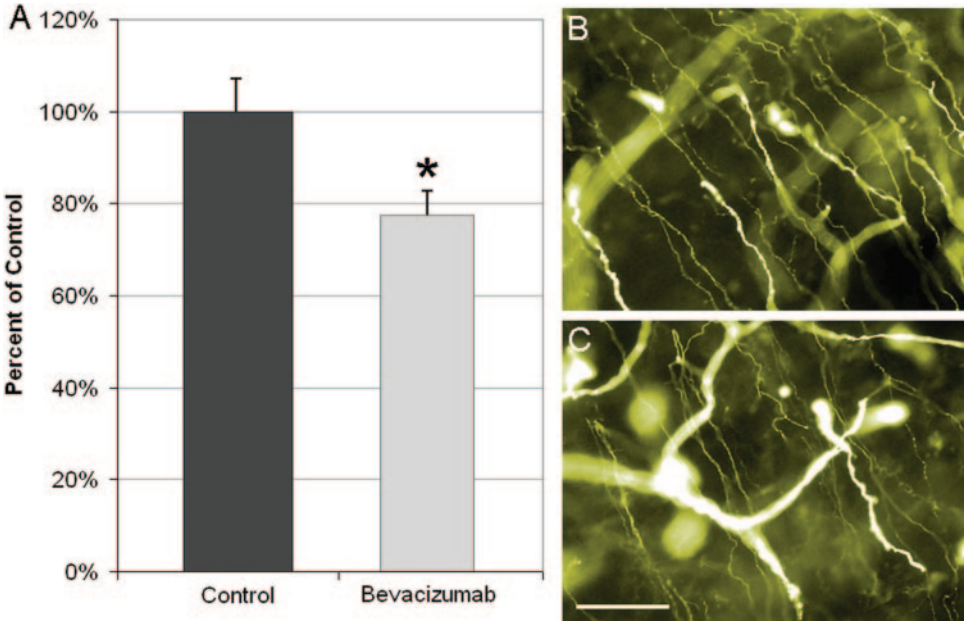

FIGURE 11. Effect of anti–VEGF antibody on corneal nerve regeneration in vivo. Mice with corneal de-epithelialization wounds were treated with corneal hydrations of 25 mg/mL mouse IgG or 25 mg/mL bevacizumab. After 3 days, mice were killed and corneas were excised and photographed for neurofluorescence, as in Figure 1. Corneas treated with bevacizumab (**C**; $n = 7$) recovered to a neuron density of 12,328 ± 845 $\mu m/mm^2$, whereas those given nonspecific mouse IgG (**B**; $n = 8$) recovered to a density of 15,939 ± 1141 $\mu m/mm^2$, representing a reduction in subbasal nerve density of 23% ($P < 0.03$). (**A**) Data are plotted as a percentage of control. *Asterisk*: statistical significance with $P < 0.05$. Scale bar, 100 μmScale bar, 100 μm.

of similarities in the patterning of epithelial cells and corneal nerves and data showing the epithelium expresses some VEGF receptors, it is possible that VEGF plays a role in determining epithelial cell patterning.[24,40,41] Further studies will be needed to determine which VEGF receptors are responsible for these and other actions of VEGF in the cornea.

In summary, our data indicate that the trigeminal ganglion expresses VEGF and the VEGF receptors VEGFR1, VEGFR2, NRP1, and NRP2. The cornea expresses VEGFR1, VEFR2, and NRP1. VEGF is a potent stimulant of trigeminal neuronal outgrowth in vitro, and blockage of VEGF signaling impairs regeneration of the corneal subbasal nerve plexus after injury.

Acknowledgments

The authors thank Ivan R. Schwab for his helpful insights and Crina Nimigean for critical review of the manuscript.

References

1. Marfurt CF, Ellis LC. Immunohistochemical localization of tyrosine hydroxylase in corneal nerves. *J Comp Neurol*. 1993;336:517–531.
2. Muller LJ, Vrensen GF, Pels L, Cardozo BN, Willekens B. Architecture of human corneal nerves. *Invest Ophthalmol Vis Sci*. 1997; 38:985–994.
3. Wilson SE, Ambrosio R. Laser in situ keratomileusis-induced neurotrophic epitheliopathy. *Am J Ophthalmol*. 2001;132:405–406.
4. Murphy CJ, Marfurt CF, McDermott A, et al. Spontaneous chronic corneal epithelial defects (SCCED) in dogs: clinical features, innervation, and effect of topical SP, with or without IGF-1. *Invest Ophthalmol Vis Sci*. 2001;42:2252–2261.
5. Robinson CJ, Stringer SE. The splice variants of vascular endothelial growth factor (VEGF) and their receptors. *J Cell Sci*. 2001;114: 853–865.
6. Sondell M, Sundler F, Kanje M. Vascular endothelial growth factor is a neurotrophic factor which stimulates axonal outgrowth through the flk-1 receptor. *Eur J Neurosci*. 2000;12:4243–4254.
7. Adamis AP, Miller JW, Bernal MT, et al. Increased vascular endothelial growth factor levels in the vitreous of eyes with proliferative diabetic retinopathy. *Am J Ophthalmol*. 1994;118:445–450.
8. Alon T, Hemo I, Itin A, Pe'er J, Stone J, Keshet E. Vascular endothelial growth factor acts as a survival factor for newly formed retinal vessels and has implications for retinopathy of prematurity. *Nat Med*. 1995;1:1024–1028.
9. Tanaka Y, Katoh S, Hori S, Miura M, Yamashita H. Vascular endothelial growth factor in diabetic retinopathy. *Lancet*. 1997;349:1520.
10. Lashkari K, Hirose T, Yazdany J, McMeel JW, Kazlauskas A, Rahimi N. Vascular endothelial growth factor and hepatocyte growth factor levels are differentially elevated in patients with advanced retinopathy of prematurity. *Am J Pathol*. 2000;156:1337–1344.
11. Jonas JB, Neumaier M. Vascular endothelial growth factor and basic fibroblast growth factor in exudative age-related macular degeneration and diffuse diabetic macular edema. *Ophthalmic Res*. 2007;39:139–142.
12. Waisbourd M, Loewenstein A, Goldstein M, Leibovitch I. Targeting vascular endothelial growth factor: a promising strategy for treating age-related macular degeneration. *Drugs Aging*. 2007;24:643–662.
13. Ambati BK, Nozaki M, Singh N, et al. Corneal avascularity is due to soluble VEGF receptor-1. *Nature*. 2006;443:993–997.
14. Amano S, Rohan R, Kuroki M, Tolentino M, Adamis AP. Requirement for vascular endothelial growth factor in wound- and inflammation-related corneal neovascularization. *Invest Ophthalmol Vis Sci*. 1998;39:18–22.
15. Bock F, Onderka J, Dietrich T, et al. Bevacizumab as a potent inhibitor of inflammatory corneal angiogenesis and lymphangiogenesis. *Invest Ophthalmol Vis Sci*. 2007;48:2545–2552.
16. Sondell M, Lundborg G, Kanje M. Vascular endothelial growth factor has neurotrophic activity and stimulates axonal outgrowth, enhancing cell survival and Schwann cell proliferation in the peripheral nervous system. *J Neurosci*. 1999;19:5731–5740.
17. Bocker-Meffert S, Rosenstiel P, Rohl C, et al. Erythropoietin and VEGF promote neural outgrowth from retinal explants in postnatal rats. *Invest Ophthalmol Vis Sci*. 2002;43:2021–2026.
18. Nishijima K, Ng YS, Zhong L, et al. Vascular endothelial growth factor-A is a survival factor for retinal neurons and a critical neuroprotectant during the adaptive response to ischemic injury. *Am J Pathol*. 2007;171:53–67.
19. Sun Y, Jin K, Xie L, et al. VEGF-induced neuroprotection, neurogenesis, and angiogenesis after focal cerebral ischemia. *J Clin Invest*. 2003;111:1843–1851.
20. Carmeliet P. Angiogenesis in health and disease. *Nat Med*. 2003; 9:653–660.
21. Lambrechts D, Storkebaum E, Morimoto M, et al. VEGF is a modifier of amyotrophic lateral sclerosis in mice and humans and protects motoneurons against ischemic death. *Nat Genet*. 2003;34:383–394.
22. Storkebaum E, Carmeliet P. VEGF: a critical player in neurodegeneration. *J Clin Invest*. 2004;113:14–18.
23. Inan UU, Avci B, Kusbeci T, Kaderli B, Avci R, Temel SG. Preclinical safety evaluation of intravitreal injection of full-length humanized vascular endothelial growth factor antibody in rabbit eyes. *Invest Ophthalmol Vis Sci*. 2007;48:1773–1781.
24. Yu CQ, Rosenblatt MI. Transgenic corneal neurofluorescence in mice: a new model for in vivo investigation of nerve structure and regeneration. *Invest Ophthalmol Vis Sci*. 2007;48:1535–1542.
25. Kawakita T, Espana EM, He H, Yeh LK, Liu CY, Tseng SC. Calcium-induced abnormal epidermal-like differentiation in cultures of mouse corneal-limbal epithelial cells. *Invest Ophthalmol Vis Sci*. 2004;45:3507–3512.
26. Guan F, Villegas G, Teichman J, Mundel P, Tufro A. Autocrine class 3 semaphorin system regulates slit diaphragm proteins and podocyte survival. *Kidney Int*. 2006;69:1564–1569.
27. Saint-Geniez M, Maldonado AE, D'Amore PA. VEGF expression and receptor activation in the choroid during development and in the adult. *Invest Ophthalmol Vis Sci*. 2006;47:3135–3142.
28. Jackson MW, Bentel JM, Tilley WD. Vascular endothelial growth factor (VEGF) expression in prostate cancer and benign prostatic hyperplasia. *J Urol*. 1997;157:2323–2328.
29. Cackowski FC, Xu L, Hu B, Cheng SY. Identification of two novel alternatively spliced Neuropilin-1 isoforms. *Genomics*. 2004;84:82–94.
30. Rozsa AJ, Guss RB, Beuerman RW. Neural remodeling following experimental surgery of the rabbit cornea. *Invest Ophthalmol Vis Sci*. 1983;24:1033–1051.
31. Chan KY, Jarvelainen M, Chang JH, Edenfield MJ. A cryodamage model for studying corneal nerve regeneration. *Invest Ophthalmol Vis Sci*. 1990;31:2008–2021.
32. Trabucchi G, Brancato R, Verdi M, Carones F, Sala C. Corneal nerve damage and regeneration after excimer laser photokeratectomy in rabbit eyes. *Invest Ophthalmol Vis Sci*. 1994;35:229–235.
33. Cavallotti C, Gherardi F, Artico M, Pescosolido N, Feher J, Balacco Gabrieli C. Catecholaminergic nerve fibres in normal and alkali-burned rabbit cornea. *Can J Ophthalmol*. 1998;33:259–263.
34. de Leeuw AM, Chan KY. Corneal nerve regeneration: correlation between morphology and restoration of sensitivity. *Invest Ophthalmol Vis Sci*. 1989;30:1980–1990.
35. Esquenazi S, Bazan HE, Bui V, He J, Kim DB, Bazan NG. Topical combination of NGF and DHA increases rabbit corneal nerve regeneration after photorefractive keratectomy. *Invest Ophthalmol Vis Sci*. 2005;46:3121–3127.
36. Hong YK, Lange-Asschenfeldt B, Velasco P, et al. VEGF-A promotes tissue repair-associated lymphatic vessel formation via VEGFR-2 and the $\alpha 1\beta 1$ and $\alpha 2\beta 1$ integrins. *FASEB J*. 2004;18:1111–1113.
37. Senger DR, Claffey KP, Benes JE, Perruzzi CA, Sergiou AP, Detmar M. Angiogenesis promoted by vascular endothelial growth factor: regulation through $\alpha 1\beta 1$ and $\alpha 2\beta 1$ integrins. *Proc Natl Acad Sci U S A*. 1997;94:13612–13617.
38. Yu L, Wu X, Cheng Z, et al. Interaction between bevacizumab and murine VEGF-A: a reassessment. *Invest Ophthalmol Vis Sci*. 2008; 49:522–527.
39. Cursiefen C, Chen L, Saint-Geniez M, et al. Nonvascular VEGF receptor 3 expression by corneal epithelium maintains avascularity and vision. *Proc Natl Acad Sci U S A*. 2006;103:11405–11410.
40. Nagasaki T, Zhao J. Centripetal movement of corneal epithelial cells in the normal adult mouse. *Invest Ophthalmol Vis Sci*. 2003; 44:558–566.
41. Dvorscak L, Marfurt CF. Age-related changes in rat corneal epithelial nerve density. *Invest Ophthalmol Vis Sci*. 2008;49:910–916.